AP1G mediates vacuolar acidification during synergid-controlled pollen tube reception

Jia-Gang Wang[a,1], Chong Feng[a,1], Hai-Hong Liu[a], Qiang-Nan Feng[a], Sha Li[a], and Yan Zhang[a,2]

[a]State Key Laboratory of Crop Biology, College of Life Sciences, Shandong Agricultural University, Tai'an, 271018, China

Edited by Robert L. Fischer, University of California, Berkeley, CA, and approved April 18, 2017 (received for review October 28, 2016)

Double fertilization in angiosperms requires the delivery of immotile sperm through pollen tubes, which enter embryo sacs to initiate synergid degeneration and to discharge. This fascinating process, called pollen tube reception, involves extensive communications between pollen tubes and synergids, within which few intracellular regulators involved have been revealed. Here, we report that vacuolar acidification in synergids mediated by AP1G and V-ATPases might be critical for pollen tube reception. Functional loss of *AP1G* or *VHA-A*, encoding the γ subunit of adaptor protein 1 or the shared component of two endomembrane V-ATPases, respectively, impaired synergid-controlled pollen tube reception and caused partial female sterility. AP1G works in parallel to the plasma membrane-associated receptor FERONIA in synergids, suggesting that synergid-mediated pollen tube reception requires proper sorting of vacuolar cargos by AP1G. Although AP1G did not mediate the targeting of V-ATPases, *AP1G* loss of function or the expression of AP1G-RNAi compromised vacuolar acidification mediated by V-ATPases, implying their genetic interaction. We propose that vacuolar acidification might represent a distinct cell-death mechanism specifically adopted by the plant phylum, which is critical for synergid degeneration during pollen tube reception.

adaptor protein 1 | pollen tube reception | vacuolar trafficking | vacuolar acidification | cell death

Double fertilization in angiosperm is preceded by fine-tuned communication between male and female gametophytes (1, 2). The female gametophyte (FG), i.e., the embryo sac, is formed inside the ovules and contains an egg cell, a central cell, two synergid cells, and three antipodal cells (3). Upon landing on a receptive pistil, a pollen grain forms a long cylindrical extension, called a pollen tube, which extends inside female sporophytic tissues. To deliver immotile sperm, pollen tubes perceive attractive signals sent out by the FG, change their growth axis, and finally enter the embryo sacs through the micropyle (1–4). A process called "pollen tube reception" instructs the cessation and discharge of the penetrating pollen tube, leading to sperm release and fertilization (1–4).

Studies have uncovered key female factors controlling pollen tube reception, including FERONIA (FER) (5–7), LORELEI (LRE) (8, 9), and early nodulin-like proteins (ENODLs) (10) and NORTIA (NTA) (11). These synergid receptors likely operate in the same genetic pathway (10–12) whose functional loss caused the failure of pollen tube discharge and led to reduced female fertility (5–9, 11). Male ligands are yet to be identified. However, recent studies showed that the production of reactive oxygen species (ROS) and Ca^{2+} spiking are downstream events of FER-controlled pollen tube reception (13–16).

Synergid degeneration, a form of programmed cell death (PCD), is a key step during pollen tube reception. Between the two synergid cells, a receptive synergid cell is the one that succeeds in interacting with the pollen tube and induces it to burst and undergoes cell death first. The other synergid cell that continues to persist and then undergoes cell death orchestrated by the fertilized egg cell and the central cell is the persistent synergid (3, 11, 17). In *Arabidopsis*, the degeneration of the receptive synergid usually accompanies the discharge of the incoming pollen tube (18). Synergid degeneration can also be initiated without pollen tube discharge (17). The degeneration and removal of the persistent synergid are mediated by ethylene signaling and the central cell (19, 20).

We report here that vacuolar acidification mediated by AP1G and V-ATPases might be critical for synergid-controlled pollen tube reception. AP1 is a tetrameric protein complex regulating protein sorting at the *trans*-Golgi network/early endosome (TGN/EE), the convergent compartment for anterograde and retrograde trafficking pathways. AP1γ (AP1G) is encoded by *AP1G1* and *AP1G2*. Single mutants of either *AP1G1* or *AP1G2* did not have a discernible phenotype. However, functional loss of both genes resulted in partial female sterility due to the failure of pollen tube discharge and synergid degeneration. Although AP1G mediates protein sorting at the TGN/EE both to the plasma membrane (PM) and the tonoplast, *AP1G* loss of function caused mistargeting of tonoplast proteins but not that of FER. In addition, AP1G and FER are genetically independent in controlling pollen tube reception. These results suggested that AP1G functions in synergids through mediating vacuolar trafficking. We further showed that abolishing the activity of V-ATPases compromised vacuolar acidification and caused a similar defect in pollen tube reception. Finally, we demonstrate that AP1G is critical for synergid vacuolar acidification, possibly by mediating the activities of V-ATPases. Our results suggested that vacuolar acidification, contributed by AP1G and V-ATPases, is involved in synergid degeneration and pollen tube reception. Vacuolar acidification-mediated cell degeneration may represent a distinct cell-death mechanism adopted specifically by the plant kingdom.

Results

Functional Loss of *AP1G* Reduces Fertility. To determine the function of *AP1G*s *in planta*, we analyzed mutants for *AP1G1* and *AP1G2* (Fig. 1*A*). Single mutants showed no discernible phenotype (Fig. 1 *D* and *E* and Fig. S1). We thus crossed the null alleles, *ap1g1-1* and *ap1g2-1*, to generate a double knockout line. Plants with the genotype *ap1g1-1/ap1g1-1;AP1G2/ap1g2-1* (*ap1g1 g2*/+) but not those with the genotype *AP1G1/ap1g1-1;*

Significance

Double fertilization of angiosperms is preceded by the death of gametophytic cells: Two synergid cells degenerate to create a microenvironment for fertilization, whereas the pollen tube bursts to discharge sperm cells. This process is called pollen tube reception, in which a few synergid surface proteins have been identified, but intracellular activities involved are obscure. We report here that vacuolar acidification, mediated by V-ATPases and adaptor protein 1, might be an important mechanism for synergid degeneration during pollen tube reception. The study provides insights into a cell-death mechanism specifically adopted by the plant phylum.

Author contributions: J.-G.W., C.F., H.-H.L., and Q.-N.F. performed research; Q.-N.F. and S.L. contributed new reagents/analytic tools; J.-G.W., C.F., Q.-N.F., S.L., and Y.Z. analyzed data; and Y.Z. wrote the paper.

The authors declare no conflict of interest.

This article is a PNAS Direct Submission.

[1]J.-G.W. and C.F. contributed equally to this work.

[2]To whom correspondence should be addressed. Email: yzhang@sdau.edu.cn.

This article contains supporting information online at www.pnas.org/lookup/suppl/doi:10.1073/pnas.1617967114/-/DCSupplemental.

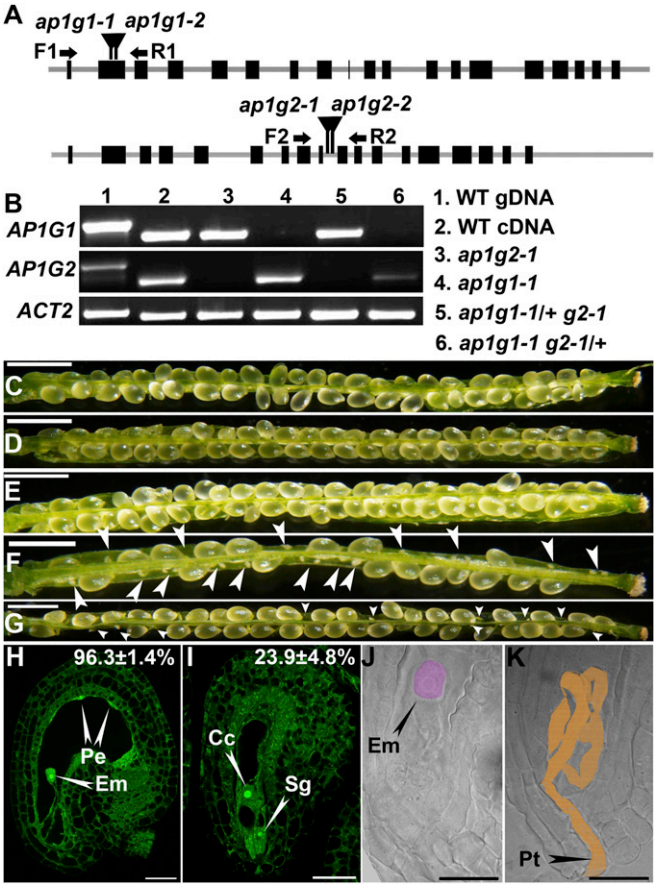

Fig. 1. *AP1G* loss of function reduced fertility. (*A*) Schematic illustration of T-DNA insertions within *AP1Gs* (*AP1G1* and *AP1G2*). Filled boxes indicate coding regions. Arrows indicate the binding regions for RT-PCR primers. (*B*) Transcript analysis showing that both *ap1g1-1* and *ap1g2-1* are null mutants. *ACT2* (*ACTIN2*) was used as the internal control. (*C*–*G*) Seed set analyses in self-fertilized WT (*C*), *ap1g1-1* (*D*), *ap1g2-1* (*E*), the *trans*-heterozygous mutant *ap1g1 g2*/+ (*F*), and *ap1g1*/+ *g2* (*G*). Results are means ± SD (n = 100). Seed sets of *ap1g1*/+ *g2* and *ap1g1 g2*/+ are significantly different from WT or either single mutant (one-way ANOVA, Tukey–Kramer test, $P < 0.05$). Arrowheads point at unfertilized ovules. (*H* and *I*) CLSM of ovules at 24 HAP either from WT (*H*) or from *ap1g1*/+ *g2* (*I*). Data shown on the top right indicate the average percentage of the displayed category. Results shown are means ± SEs (SEM) of 10 replicates. Wild type and *ap1g1*/+ *g2* are significantly different (*t* test, $P < 0.05$). (*J* and *K*) Differential interference contrast images showing an embryo (pseudocolored pink) at 24 HAP from WT (*J*) or an embryo sac from *ap1g1*/+ *g2* with an overgrown pollen tube (*K*, pseudocolored light brown). Cc, central cell; Em, embryo; Pe, peripheral endosperm; Pt, pollen tube; Sg, synergid. (Scale bars: *C*–*G*, 500 μm; *H* and *I*, 25 μm; *J* and *K*, 20 μm.)

ap1g2-1/*ap1g2-1* (*ap1g1*/+ *g2*) were dwarf and bushy (Fig. S1), possibly due to haplo-insufficiency, because the expression of *AP1G1* is higher than that of *AP1G2* in most tissues (21). A significant portion of *ap1g1*/+ *g2* or *ap1g1 g2*/+ ovules did not grow, compared with that in wild type (WT) or in the single mutants (Fig. 1 *C*–*G*). To determine whether these ovules were unfertilized or defective in embryogenesis, we analyzed these ovules 24 h after pollination (HAP) by confocal laser scanning microscopy (CLSM) and after whole-mount ovule clearing. Almost all wild-type ovules and approximately 75% of *ap1g1*/+ *g2* ovules contained an embryo and peripheral endosperm (Fig. 1 *H* and *J* and Table S1), indicative of fertilization. However, approximately 25% *ap1g1*/+ *g2* ovules contained a central cell and egg cell at 24 HAP (Fig. 1*I* and Table S1), indicative of failed fertilization. The unfertilized *ap1g1*/+ *g2* ovules contained entangled pollen tubes (Fig. 1*K*), whereas they ceased growth and discharge contents in WT.

No double homozygous plants were obtained from self-pollinated *ap1g1*/+ *g2* or *ap1g1 g2*/+ (Table S2). Segregation ratios from reciprocal crosses showed that *ap1g1 g2* was male gametophytic lethal and partially defective in female gametophytic transmission (Table S2). Because of the haplo-insufficient phenotype of *ap1g1 g2*/+ in vegetative tissue development (Fig. S1), most of our following studies used *ap1g1*/+ *g2* (hereafter as *ap1g*/+) to avoid the influence of poor vegetative growth. However, either gene driven by the Pro_{UBQ10} promoter fully complemented the mutant phenotype (Fig. S1), indicating that the two genes are functionally interchangeable.

Impaired Pollen Tube Reception in the FG of *ap1g*/+. To determine the cause of reduced female transmission of *ap1g*, we first introduced Pro_{ES1}:NLS-YFP into WT or *ap1g*/+ and examined the development of the FG. Because Pro_{ES1} is active in all cells of the FGs (22), the nucleus-targeting YFP (NLS-YFP) driven by Pro_{ES1} should show FGs with seven nuclei. CLSM on unfertilized mature ovules at flower stage 12 indicated that the position of synergid cells and the organization of FG were comparable between WT and *ap1g*/+ (Fig. S2), indicating that *AP1G*s were not essential for FG development.

Next, we hand-pollinated emasculated wild-type or *ap1g*/+ pistils with Pro_{LAT52}:GUS pollen; histochemical GUS staining showed a slight reduction of pollen tube attraction in *ap1g*/+ pistils (Fig. 2 *A* and *B* and Table S1). Aniline blue staining of WT or *ap1g*/+ pistils at 48 HAP showed that a significant portion (36.3 ± 10.8%) of *ap1g*/+

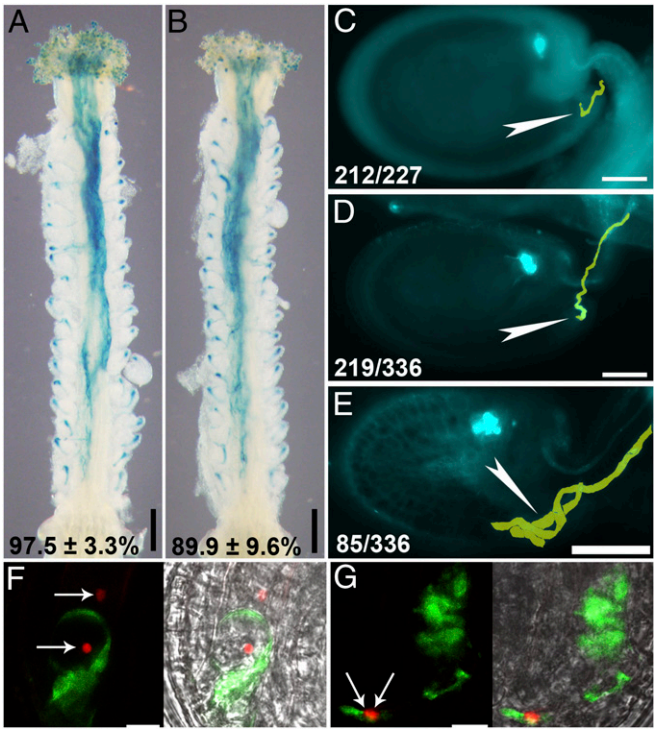

Fig. 2. Female gametophytes of *ap1g1 g2* are compromised in pollen tube reception. (*A* and *B*) Representative histochemical GUS analysis of wild-type (*A*) or $ap1g1^{+/-}$ *g2* (*B*) pistils emasculated and hand-pollinated with Pro_{LAT52}:GUS pollen at 12 HAP. Results shown at the bottom are means ± SD, n = 25. (*C*–*E*) Representative aniline blue-stained WT ovule (*C*), $ap1g1^{+/-}$ *g2* ovule with normal pollen tube reception (*D*), $ap1g1^{+/-}$ *g2* ovule with a tangled pollen tube (*E*) at 48 HAP. Pollen tubes are pseudocolored in yellow. Arrowheads point at the micropyle. At the bottom: displayed ovules/all ovules examined. (*F* and *G*) CLSM of a wild-type (*F*) or *ap1g1 g2* (*G*) embryo sac invaded by a Pro_{LAT52}:GFP;Pro_{HTR10}:HTR10-mRFP pollen tube. The right images are merges of GFP, RFP, and BF channels. Arrows in *F* and *G* indicate the position of sperm cells. (Scale bars: *A* and *B*, 200 μm; *C*–*E*, 50 μm; *F* and *G*, 10 μm.)

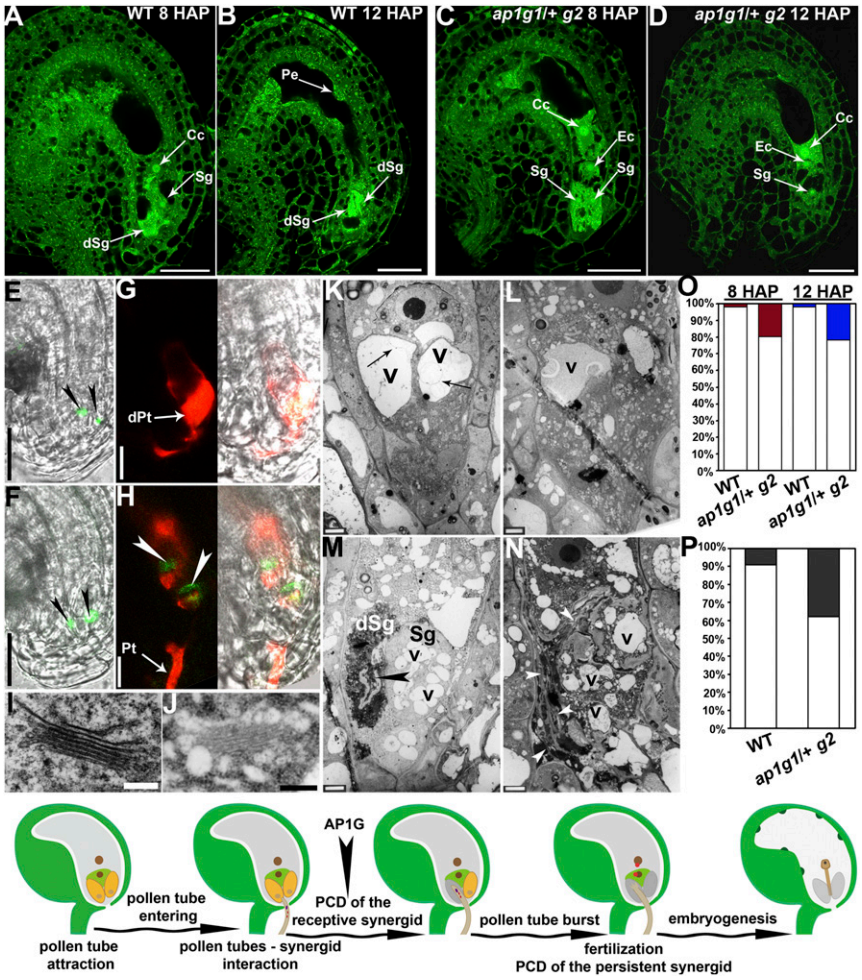

Fig. 3. Synergid degeneration induced by pollen tube arrival is compromised by *AP1G* loss of function. (*A–D*) CLSM images of ovules from WT (*A* and *B*) or *ap1g1/+ g2* (*C* and *D*) emasculated and hand-pollinated with wild-type pollen at 8 HAP (*A* and *C*) or 12 HAP (*B* and *D*). Image shown in *C* is projection of three confocal images taken at different focal planes to show the presence of different nuclei. (*E–H*) CLSM image of ovules from Pro_{DD39}:NLS-YFP (*E* and *G*) or Pro_{DD39}:NLS-YFP; *ap1g1/+ g2* (*F* and *H*) before pollination (*E* and *F*) or pollinated with a Pro_{LAT52}:DsRed pollen tube at 8 HAP (*G* and *H*). The transgene Pro_{DD39}:NLS-YFP is present as homozygous single copy in both WT and *ap1g1/+ g2*. Arrowheads indicate synergid nuclei. Images in *E* and *F* are merges of GFP and bright-field (BF) channels. Images shown in *G* and *H* are merges of GFP/RFP channels and merges of GFP/RFP/BF channels. (*I* and *J*) TEM of a Golgi stack in a wild-type (*I*) or a presumble *ap1g1 g2* synergid (*J*). (*K–N*) TEM of a wild-type (*K* and *M*) or a presumble *ap1g1 g2* (*L* and *N*) embryo sac before pollination (*K* and *L*) or upon pollen tube entrance (*M* and *N*). Arrows in *K* indicate invaginated or convoluted vacuolar membrane inside the central vacuole of a synergid. Arrowhead in *M* indicates a discharging pollen tube. Arrowheads in *N* point at an overgrown pollen tube. (*O*) Quantitative analyses of synergid degeneration by CLSM. Percentage of ovules containing one synergid degenerated at 8 HAP or two synergids degenerated at 12 HAP is shown with open columns, whereas filled columns indicate the percentage of ovules containing two intact synergids at 8 HAP (red) or one intact synergid at 12 HAP (blue). (*P*) Percentage of discharging (empty columns) or nondischarging (filled columns) Pro_{LAT52}:DsRed pollen tubes at 12 HAP. In total, 25 pistils were analyzed for each genotype and all showed similar results. (*Q*) A cartoon model illustrating the steps leading to fertilization. Arrowhead indicates the timing of *AP1G* action in these processes. Cc, central cell; dSg, degenerated synergid; dPt, discharged pollen tube; Ec, egg cell; Pe, peripheral endosperm; Pt, pollen tube; Sg, synergid; v, vacuoles. (Scale bars: *A–F*, 25 μm; *G* and *H*, 10 μm; *I* and *J*, 200 nm; *K–N*, 2 μm.)

ovules were unfertilized (Table S1), in contrast to that in WT (Table S1). Overgrown pollen tubes were present in unfertilized ovules (85 of 117; Fig. 2*E*), indicating impaired pollen tube reception (5–7, 9, 11, 23, 24).

To verify the impaired pollen tube reception, we hand-pollinated emasculated wild-type or *ap1g*/+ pistils with Pro_{LAT52}:GFP; Pro_{HTR10}:HTR10-mRFP pollen, in which sperm nuclei are labeled with mRFP and pollen tubes express cytoplasmic GFP (25). Pollen tubes discharged their content, that is, cytoplasm and sperm cells (67 of 79; Fig. 2*F*) upon arrival in WT. However, 18 of 75 *ap1g*/+ FGs contained a nondischarging pollen tube (Fig. 2*G*). As a result, sperm cells were trapped way back in pollen tubes rather than being released into the FG (Fig. 2*G*). These results demonstrated a critical role of *AP1G* in FG-controlled pollen tube reception.

Pollen Tube Arrival–Induced Synergid Degeneration Is Impaired by *AP1G* Loss of Function. To determine how *AP1G* loss of function caused abnormal tube reception, we first used CLSM to examine wild-type and *ap1g*/+ pistils at 8 HAP or 12 HAP. As reported (18, 26), the receptive synergid degenerated at 8 HAP, whereas the persistent synergid degenerated at 12 HAP in most wild-type ovules (Fig. 3 *A*, *B*, and *O*). The appearance of peripheral endosperm also indicated successful fertilization (Fig. 3*B*). By contrast, a notable portion of *ap1g*/+ ovules contained two synergids at 8 HAP or one synergid at 12 HAP (Fig. 3 *C, D*, and *O*). Accordingly, autofluorescence from degenerating synergids as seen in WT at a comparable stage was undetectable and peripheral endosperm was not present in those *ap1g*/+ ovules (Fig. 3*D*). These results supported a role of *AP1G* in synergid degeneration induced by pollen tube arrival.

To confirm that synergid degeneration was not properly executed upon pollen tube arrival by *AP1G* loss of function, we expressed NLS-YFP under a synergid-specific promoter Pro_{DD39} (27). Synergid nuclei were labeled in both unfertilized wild-type and *ap1g*/+ ovules (Fig. 3 *E* and *F*). Pollination with Pro_{LAT52}:DsRed pollen at 12 HAP led to pollen tube discharge and undetectable NLS-YFP signals in WT (Fig. 3 *G* and *P*), indicative of synergid death. By contrast, ovules from the Pro_{DD39}:NLS-YFP;*ap1g*/+ plants contained a nondischarging, overgrowing pollen tube wrapping around two synergid nuclei (17 of 72; Fig. 3 *H* and *P*).

To gain further evidence for the role of *AP1G*s in synergid degeneration, we performed transmission electron microscopy (TEM) on mature pistils before pollination or at 8 HAP. In mature wild-type embryo sacs, synergid cells contained a large central vacuole distal to the micropyle, in which few electron-dense materials were present (Fig. 3*K*). In embryo sacs with distorted Golgi morphology (Fig. 3*J*) indicative of the *ap1g* identity (28), synergid cells also contained a central vacuole distal to the micropyle (Fig. 3*L*). However, unlike those in WT (Fig. 3*K*), the central vacuoles were filled with electron-dense materials (Fig. 3*L*), suggesting defective vacuolar degradation. In addition, numerous small vacuoles were present in addition to the central vacuoles of the presumable *ap1g* synergids (Fig. 3*L*), but not in those of WT (Fig. 3*K*). At 8 HAP, pollen tube arrival in wild-type embryo sacs was accompanied with the degeneration of the receptive synergid (Fig. 3*M*). At the same time, vacuoles became fragmented with reduced membrane integrity

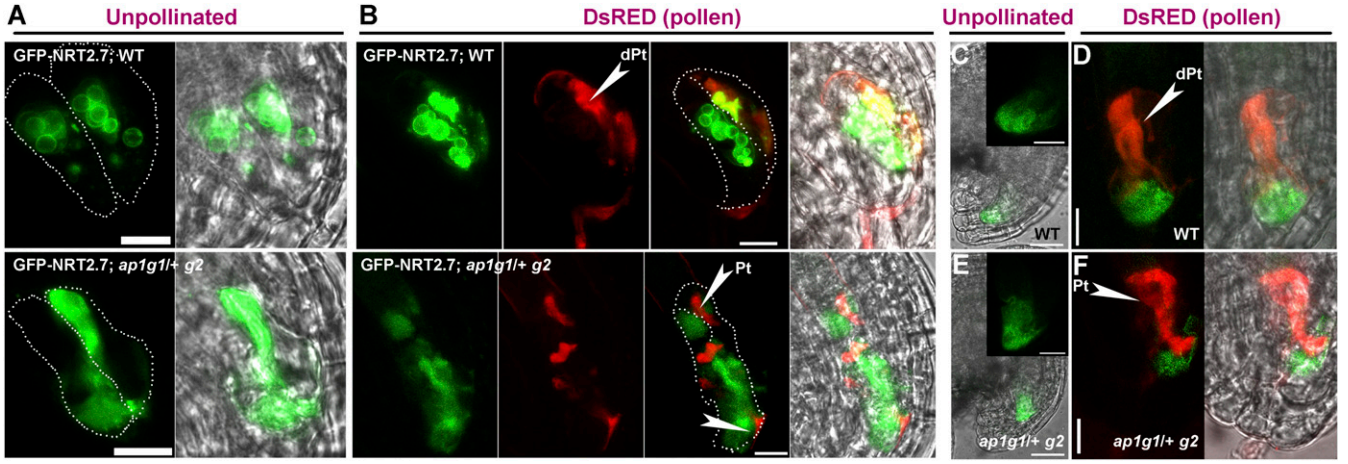

Fig. 4. Targeting of tonoplast proteins but not FERONIA the key plasma membrane receptor is interfered in synergids by *AP1G* loss of function. (*A* and *B*) CLSM of Pro_{DD39}:GFP-NRT2.7 in synergids of WT or *ap1g1*/+ *g2*. Pistils from Pro_{DD39}:GFP-NRT2.7 or Pro_{DD39}:GFP-NRT2.7;*ap1g1*/+ *g2* plants were either emasculated at maturation for visualization (*A*) or emasculated and pollinated with Pro_{LAT52}:DsRed pollen and visualized at 8 HAP (*B*). Merges of GFP, RFP, and BF channels are shown at the right side in *B*. Dotted lines illustrate synergid cells. (*C*–*F*) CLSM of Pro_{DD39}:FER-YFP in synergids of WT (*C* and *D*) or *ap1g1*/+ *g2* (*E* and *F*). Pistils from Pro_{DD39}:FER-YFP or Pro_{DD39}:FER-YFP;*ap1g1*/+ *g2* plants were either emasculated at maturation for visualization (*C* and *E*) or emasculated and pollinated with Pro_{LAT52}:DsRed pollen and visualized at 8 HAP (*D* and *F*). Merges of GFP, RFP, and BFA channels are shown at the right side in *D* and *F*. Insets in *C* and *E* are their corresponding close-ups at the micropylar region. dPt, discharged pollen tube; Pt, pollen tube. (Scale bars: *A* and *B*, 10 μm; *D* and *F* and *C* and *E*, *Inset*, 25 μm.)

of the persistent synergid (Fig. 3*M*), indicating an immediate cell death. Consistent with the results obtained by using fluorescent pollen tubes (Fig. 3*P*), nondischarging pollen tubes were observed in the presumable *ap1g* embryo sacs after pollination (Fig. 3*N*) based on the Golgi morphology (Fig. 3*J*). No synergid degeneration occurred in these embryo sacs (Fig. 3*N*). Fragmented vacuoles filled with electron-dense materials were observed in synergid cells, for which membrane integrity was well preserved (Fig. 3*N*), unlike that of WT (Fig. 3*M*). These results indicated that functional loss of *AP1G*s compromised synergid degeneration upon pollen tube arrival, which is likely crucial for pollen tube discharge (18).

To determine whether the role of *AP1G* in synergid degeneration was cell-autonomous, we confirmed their expression in ovules and synergid cells by RNA in situ hybridization and by histochemical GUS staining of their promoter-reporter lines. Both *AP1G1* and *AP1G2* were expressed in ovules, especially at the micropylar region where synergid cells are located (Fig. S3).

Mistargeting of Tonoplast Proteins by *AP1G* Functional Loss. Because *AP1G1* was reported to regulate vacuolar trafficking of tonoplast proteins (29), we attempted to examine whether AP1Gs regulated vacuolar trafficking of tonoplast proteins in synergids. To this purpose, we introduced Pro_{DD39}:GFP-NRT2.7 into WT and *ap1g*/+. Synergid-specific expression of the tonoplast-associated NRT2.7 (30) would allow us to examine the potential defects on the vacuolar trafficking of tonoplast proteins in *ap1g* synergids. In unpollinated mature wild-type ovules, GFP-NRT2.7 was localized at the tonoplast of the vacuoles (Fig. 4*A*). Upon pollen tube arrival and discharge, GFP-NRT2.7 signals formed as large aggregates in the degenerating synergid (Fig. 4*B*). By contrast, GFP-NRT2.7 was not associated with the tonoplast in a substantial portion of *ap1g*/+ ovules (Fig. 4*A* and Fig. S4). Because *AP1G* loss of function did not impair vacuolar biogenesis in synergids (Fig. 3), this result suggested impaired vacuolar delivery of NRT2.7. Upon pollination, in the *ap1g*/+ FGs that contained a nondischarging pollen tube, GFP did not show tonoplast association (Fig. 4*B*). A previously confirmed AP1G1-cargo, vacuolar ion transporter1 (VIT1) (29), showed the same pattern of distribution in the synergids of *ap1g*/+ (Fig. S4). These results indicated that vacuolar targeting of some tonoplast proteins in synergids was impaired by *AP1G* loss of function.

To exclude the possibility that defective vacuolar trafficking interfered with cellular homeostasis and, thus, impaired the targeting of PM receptors such as FER, we introduced Pro_{DD39}:FER-YFP into both WT and *ap1g*/+. In unpollinated ovules, FER distributed comparably in WT and *ap1g*/+ (Fig. 4 *C* and *E*). Pollination with Pro_{LAT52}:DsRed pollen at 12 HAP showed no differences between WT and *ap1g*/+ in FER distribution (Fig. 4

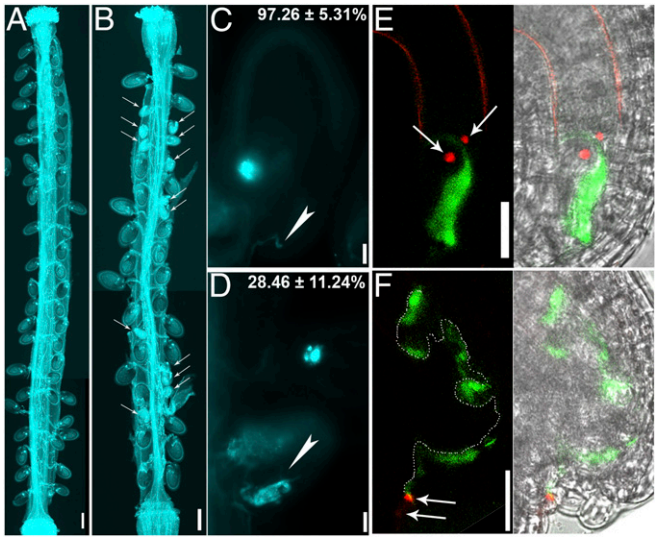

Fig. 5. Pollen tube reception is compromised in the mutant of *VHA-A*. (*A* and *B*) Aniline blue staining of wild-type pistil (*A*) or *vha-A*/+ pistil (*B*) emasculated and hand-pollinated with wild-type pollen at 48 HAP. Arrows indicate unfertilized ovules. Two to three overlapping high-magnification images were taken for one pistil. The images were then overlaid with Photoshop (Adobe Systems) to show the whole pistil. (*C* and *D*) Representative aniline blue staining of wild-type (*C*) or *vha-A*/+ (*D*) ovules at 48 HAP. Arrowheads point at micropyle in *C* and a tangled pollen tube in *D*. Percentage of the displayed category (fertilized in *C*; defective in pollen tube reception in *D*) is shown on top right of the image. Results are means ± SEM. Approximately 200 ovules were analyzed in four independent experiments. (*E* and *F*) An ovule from WT (*E*) or *vha-A*/+ plants (*F*) pollinated with Pro_{LAT52}:GFP;Pro_{HTR10}:HTR10-mRFP pollen at 12 HAP. Images shown on the left are merges of RFP and GFP channel images, whereas on the right are merges of bright-field image and fluorescence image. Dotted line in *F* indicates the growing pollen tube in the embryo sac. Arrows point at sperm cells. (Scale bars: *A* and *B*, 200 μm; *C*–*F*, 20 μm.)

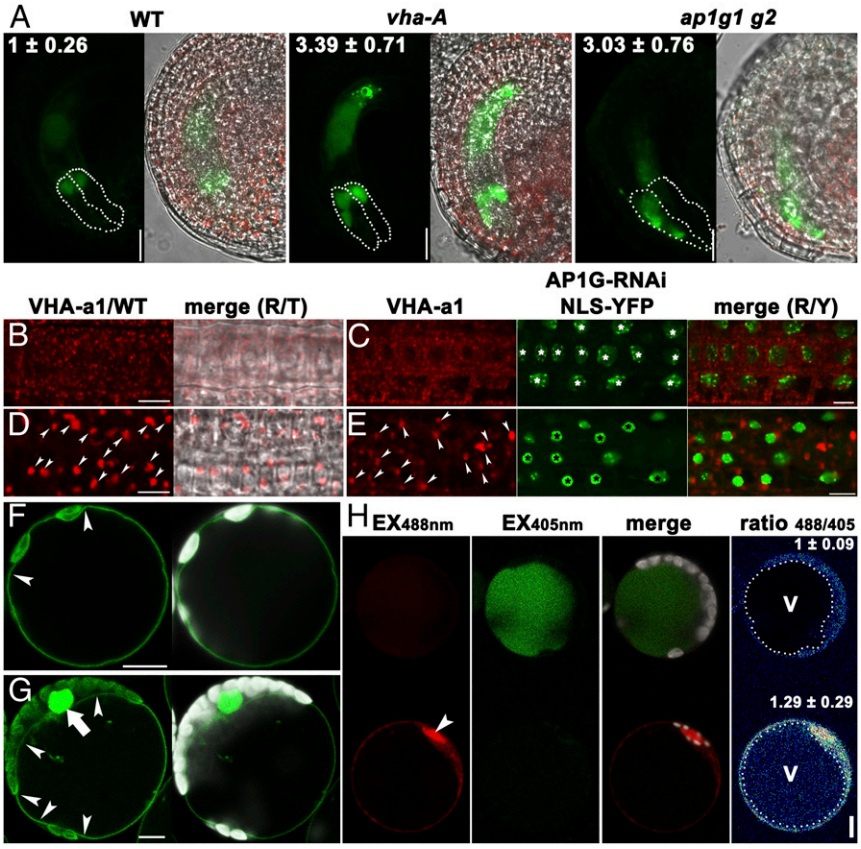

Fig. 6. *AP1G* is critical for vacuolar acidification. (*A*) CLSM of unfertilized mature ovules from the Pro_{UBQ10}:Aleu-PR (WT), Pro_{UBQ10}:Aleu-PR;*vha-A*/+ (*vha-A*), or Pro_{UBQ10}:Aleu-PR;*ap1g1*/+ *g2* (*ap1g1 g2*) transgenic plants. Numbers on the top are arbitrary intensity of Aleu-PR fluorescence in the vacuoles of synergids (highlighted with dotted lines). Results are means ± SD ($n = 30$). (*B*–*E*) CLSM of root epidermal cells from VHA-a1-RFP (*B* and *D*) or VHA-a1-RFP;Pro_{UBQ10}:AP1G-RNAi; Pro_{UBQ10}:NLS-YFP (*C* and *E*) transgenic plants with BFA treatment (*D* and *E*) or without (*B* and *C*). Arrowheads in *D* and *E* point at BFA compartments. Asterisks in *C* and *E* point at the nuclei labeled by NLS-YFP, indicative of AP1G-RNAi expression. (*F* and *G*) CLSM of an *Arabidopsis* leaf protoplast from the Pro_{35S}:VHA-a3-GFP transgenic plants (*F*) or from the Pro_{UBQ10}:AP1G-RNAi; Pro_{UBQ10}:NLS-YFP transgenic plants (*G*). Arrowheads point at the tonoplast. The arrow indicates the nucleus labeled by NLS-YFP, indicative of AP1G-RNAi expression. (*H*) Mesophyll protoplasts from the Pro_{UBQ10}:Aleu-PR transgenic plants. Emission intensities were shown in red (excitation at 488 nm, Ex488nm) or green (excitation at 405 nm, Ex405nm). The bottom one was transformed with Pro_{UBQ10}:AP1G-RNAi;Pro_{UBQ10}:NLS-YFP as indicated by the NLS-YFP–labeled nucleus (false-colored red, pointed at by an arrowhead). Pseudocolor image in the *Right* panel indicates the 488/405 nm ratio of fluorescence intensity within the vacuoles (highlighted with dotted circles). On the top right are means ± SD ($n = 30$). v, vacuole. The expression of AP1G-RNAi resulted in a significant difference in vacuolar pH (*t* test, $P < 0.01$). (Scale bars: 10 μm.)

D and *F*), suggesting that *AP1G* loss of function did not affect the distribution of key PM proteins such as FER.

To provide further evidence that FER pathway was not affected in *ap1g*/+, we introduced a null mutant of FER, *fer-4* (31), into *ap1g*/+. We were able to obtain *fer-4*/+ *ap1g*/+ plants in which both *fer-4* and *ap1g1* are heterozygous, whereas *ap1g2* was homozygous (Fig. S5). Self-fertilized *fer-4*/+ *ap1g*/+ plants produced a significantly reduced seed set compared with either *fer-4*/+ or *ap1g*/+ (Table S1). In addition, aniline blue staining of the *fer-4*/+ *ap1g*/+ pistils at 48 HAP showed that more than 75% of ovules were undeveloped, significantly different from either single mutant (Fig. S5 and Table S1). Tangled pollen tubes were detected in undeveloped ovules (Fig. S5), indicative of defective pollen tube reception. The reduced seed set and pollen tube reception of *fer-4*/+ *ap1g*/+ was a combination of *fer-4* (31) and *AP1G* loss of function (Fig. S5 and Table S1), strongly suggesting that AP1G and FER act independently in pollen tube reception.

Functional Loss of V-ATPases Phenocopies That of *AP1G* in Defective Pollen Tube Reception. Above results suggested that vacuolar trafficking from the TGN/EE was impaired by *AP1G* loss of function in synergids. *Arabidopsis VHA-A* is the single gene encoding the catalytic subunit of V-ATPases located at the TGN/EE and the tonoplast (32). Its mutation caused complete male gametophytic lethality and partial female transmission defect (32), resembling that of *AP1G*. In addition, functional loss of V-ATPases and AP1 both resulted in distorted Golgi morphology (28, 32, 33). We thus hypothesized that V-ATPases might be involved in synergid degeneration during pollen tube reception. To test this hypothesis, we analyzed the FG defects of the heterozygous mutant of *VHA-A*, *vha-A*/+ (Fig. S6). Histochemical GUS staining of *vha-A*/+ pistils pollinated with the Pro_{LAT52}:GUS pollen showed a slight reduction of pollen tube attraction in *vha-A*/+ (Fig. S7 and Table S1). A significant portion of *vha-A*/+ ovules were unfertilized and contained entangled pollen tubes at 48 HAP (Fig. 5*B*). Finally, a notable portion of *vha-A*/+ embryo sacs (15 of 83) were penetrated by a nondischarging Pro_{LAT52}:GFP;Pro_{HTR10}:HTR10-mRFP pollen tube containing unreleased sperm cells (Fig. 5 *D* and *F*), suggesting that V-ATPases are critical for synergid-controlled pollen tube reception.

Because several plant-specific PCD processes are executed by vacuolar processing enzymes (VPE) that are delivered by vacuolar trafficking and mediate vacuolar rupture (34), we thus tested whether it also participated in pollen tube arrival–induced synergid degeneration. To this purpose, we obtained a quadruple mutant of *VPE*s (*atvpe*), in which all four *Arabidopsis* VPE-coding genes were mutated (35). However, pollination assays and seed set analysis showed that *atvpe* did not show any abnormalities in pollen tube reception or fertility (Fig. S8), suggesting that synergid degeneration does not involve VPE-mediated vacuolar rupture.

Vacuolar Acidification in Synergids Is Mediated by V-ATPases and *AP1G*. The strikingly similar defects of the *vha-A*/+ and *ap1g*/+ mutants in pollen tube reception implied their genetic interaction. Because the sole function of V-ATPases is to regulate vacuolar acidification, we introduced a vacuolar pH probe, Aleu-PR (36), whose intensity negatively correlates with vacuolar acidification. By using the same confocal parameters, we found that Aleu-PR showed faint signals in the synergid vacuoles of WT (Fig. 6*A*), indicating strong vacuolar acidity. By contrast, half of the *vha-A*/+ embryo sacs contained intense Aleu-PR signals (Fig. 6*A*), indicating impaired vacuolar acidification. It was the same case for *ap1g*/+ (Fig. 6*A*) in which half of the FG were of the *ap1g1 g2* genotype, whereas the other half was of the *AP1G1 g2* genotype. To provide further evidence that *AP1G* loss of function impaired vacuolar acidification, we transformed Pro_{UBQ10}:AP1G-RNAi;Pro_{UBQ10}NLS-YFP in *Arabidopsis* protoplasts stably expressing Aleu-PR. Consistent with the results obtained from synergid vacuoles, vacuoles of the protoplasts expressing AP1G-RNAi;NLS-YFP showed a significantly higher 488 nm/405 nm

value (36) than that of WT (Fig. 6*H*), indicating compromised vacuolar acidification by the expression of AP1G-RNAi.

VHA-A is a shared component for V-ATPases at the TGN/EE and at the tonoplast, which are specified by the presence of TGN/EE-associated VHA-a1 and tonoplast-associated VHA-a2 or VHA-a3, respectively (32). To determine whether AP1G affected the targeting of V-ATPases, we examined the effect of AP1G-RNAi on the subcellular targeting of VHA-a1 and VHA-a3 by using root epidermal cells or protoplasts because synergid signals were difficult to image. As reported (37), VHA-a1 was distributed at cytosolic vesicles (Fig. 6*B*) sensitive to BFA (Fig. 5*D*), indicative of its TGN/EE identity. Expression of AP1G-RNAi;NLS-YFP did not detectably alter the TGN/EE distribution of VHA-a1 (Fig. 6 *C* and *D*). Similarly, the tonoplast-specific targeting of VHA-a3 was not affected by AP1G-RNAi; NLS-YFP (Fig. 6 *F* and *G*). These results suggested that AP1G was not involved in the subcellular targeting of V-ATPases.

Discussion

We show here that AP1G is crucial for synergid-controlled pollen tube reception. The *ap1g*/+ FGs were penetrated by nondischarging pollen tubes, a typical feature of defective pollen tube reception. CLSM of ovules at different HAP showed that synergid degeneration was impaired by *AP1G* loss of function, which is further supported by that fact that nondischarging pollen tubes always correlated with the failure of synergid degeneration. However, synergid degeneration could be initiated without pollen tube discharge (17), which explains the comparable ratio of ovules with two intact synergids at 8 HAP and one intact synergid at 12 HAP within *ap1g*/+ pistils. The impaired degeneration of the remaining synergid in *ap1g*/+ might be a secondary effect due to the failure of pollen tube discharge (23, 24). Although as a fertilization recovery strategy after defective sperm cell release, nondegenerating synergids keep sending out attractive signals for pollen tubes (26, 38), no supernumerary pollen tubes were observed in *ap1g*/+ FGs likely due to reduced pollen tube guidance.

We propose that AP1G mediates synergid degeneration during pollen tube reception through V-ATPases. First, functional loss of V-ATPases resulted in defective pollen tube reception, similar to that of *AP1G*. Second, *ap1g* synergids have a vacuolar pH comparable to that of *vha-A*. Third, genetic interference of *AP1G* by RNAi impaired vacuolar acidification in mesophyll protoplasts. Because V-ATPases are directly responsible for vacuolar acidification (39), whereas AP1G functions through mediating protein sorting at the TGN/EE to the tonoplast, it is more feasible that V-ATPases are genetically downstream of AP1G.

The next obvious question was how AP1G regulates V-ATPases to mediate vacuolar acidification. A recent study indicated that vacuolar acidification is collectively contributed by the TGN/EE-associated and the tonoplast-associated V-ATPases (40). Thus, the effect of *VHA-A* loss of function could be from the TGN/EE and the vacuoles (39). Tonoplast targeting of NRT2.7 and VIT1 was disrupted by *AP1G* functional loss, implying the key role of vacuolar trafficking in pollen tube reception. However, our results showed that the subcellular localization of both VHA-a1 and VHA-a3 was not detectably affected by genetic interference of *AP1G*. An alternative, which requires further investigation, is that AP1G may affect the activity of V-ATPases by mediating the targeting of some regulatory proteins along the vacuolar trafficking route.

Because of its specific feature compared with metazoan lysosomes, vacuole participates in plant cell death in two ways. One is through vacuolar membrane collapse to release hydrolytic enzymes in the cytosol, whereas the other is through fusion of the tonoplast and the PM (34). Because the quadruple mutant of *VPE*, which encode key proteins involved in vacuolar rupture-mediated plant PCD (34, 35), was comparably with WT during pollen tube reception, vacuolar rupture during pollen tube arrival as detected by TEM and CLSM is more likely an effect rather than the cause of synergid degeneration. Then, how vacuolar acidification may initiate synergid cell death is an intriguing question. Proton homeostasis affects endomembrane trafficking (39). Thus, defective vacuolar acidification may have compromised vesicular trafficking, leading to impaired cell death of synergids. However, the distribution of FER as the key receptor was not affected, suggesting that post-Golgi secretion was not compromised by defective vacuolar acidification. A more likely scenario is that proton homeostasis affects ROS and Ca^{2+} spiking, which have recently been shown to mediate pollen tube reception (13–16).

Materials and Methods

Details on materials and methods, including the plant material and chemicals, plasmid construction, confocal imaging, and other analyses and tools used are provided in *SI Materials and Methods*.

ACKNOWLEDGMENTS. We thank Profs. Gregory Copenhaver for Pro_{LAT52}:DsRed, Frédéric Berger for Pro_{HTR10}:HTR10-mRFP, Liwen Jiang for Aleu-PR, Alice Cheung for *fer-4*, Lei Ge for the VHA-a1:RFP lines, and Prof. Sheila McCormick for the English editing of the manuscript.

1. Johnson MA, Preuss D (2002) Plotting a course: Multiple signals guide pollen tubes to their targets. *Dev Cell* 2:273–281.
2. Kessler SA, Grossniklaus U (2011) She's the boss: Signaling in pollen tube reception. *Curr Opin Plant Biol* 14:622–627.
3. Drews GN, Yadegari R (2002) Development and function of the angiosperm female gametophyte. *Annu Rev Genet* 36:99–124.
4. Berger F, Hamamura Y, Ingouff M, Higashiyama T (2008) Double fertilization - caught in the act. *Trends Plant Sci* 13:437–443.
5. Escobar-Restrepo JM, et al. (2007) The FERONIA receptor-like kinase mediates male-female interactions during pollen tube reception. *Science* 317:656–660.
6. Huck N, Moore JM, Federer M, Grossniklaus U (2003) The *Arabidopsis* mutant *feronia* disrupts the female gametophytic control of pollen tube reception. *Development* 130:2149–2159.
7. Rotman N, et al. (2003) Female control of male gamete delivery during fertilization in *Arabidopsis thaliana*. *Curr Biol* 13:432–436.
8. Tsukamoto T, Qin Y, Huang Y, Dunatunga D, Palanivelu R (2010) A role for LORELEI, a putative glycosylphosphatidylinositol-anchored protein, in *Arabidopsis thaliana* double fertilization and early seed development. *Plant J* 62:571–588.
9. Capron A, et al. (2008) Maternal control of male-gamete delivery in *Arabidopsis* involves a putative GPI-anchored protein encoded by the *LORELEI* gene. *Plant Cell* 20:3038–3049.
10. Hou Y, et al. (2016) Maternal ENODLs are required for pollen tube reception in *Arabidopsis*. *Curr Biol* 26:2343–2350.
11. Kessler SA, et al. (2010) Conserved molecular components for pollen tube reception and fungal invasion. *Science* 330:968–971.
12. Li C, et al. (2015) Glycosylphosphatidylinositol-anchored proteins as chaperones and co-receptors for FERONIA receptor kinase signaling in Arabidopsis. *eLife* 4:4.
13. Duan Q, et al. (2014) Reactive oxygen species mediate pollen tube rupture to release sperm for fertilization in *Arabidopsis*. *Nat Commun* 5:3129.
14. Denninger P, et al. (2014) Male-female communication triggers calcium signatures during fertilization in *Arabidopsis*. *Nat Commun* 5:4645.
15. Ngo QA, Vogler H, Lituiev DS, Nestorova A, Grossniklaus U (2014) A calcium dialog mediated by the *FERONIA* signal transduction pathway controls plant sperm delivery. *Dev Cell* 29:491–500.
16. Hamamura Y, et al. (2014) Live imaging of calcium spikes during double fertilization in *Arabidopsis*. *Nat Commun* 5:4722.
17. Leydon AR, et al. (2015) Pollen tube discharge completes the process of synergid degeneration that is initiated by pollen tube-synergid interaction in Arabidopsis. *Plant Physiol* 169:485–496.
18. Sandaklie-Nikolova L, Palanivelu R, King EJ, Copenhaver GP, Drews GN (2007) Synergid cell death in Arabidopsis is triggered following direct interaction with the pollen tube. *Plant Physiol* 144:1753–1762.
19. Maruyama D, et al. (2015) Rapid elimination of the persistent synergid through a cell fusion mechanism. *Cell* 161:907–918.
20. Völz R, Heydlauff J, Ripper D, von Lyncker L, Groß-Hardt R (2013) Ethylene signaling is required for synergid degeneration and the establishment of a pollen tube block. *Dev Cell* 25:310–316.
21. Zimmermann P, Hirsch-Hoffmann M, Hennig L, Gruissem W (2004) GENEVESTIGATOR. Arabidopsis microarray database and analysis toolbox. *Plant Physiol* 136:2621–2632.
22. Pagnussat GC, Alandete-Saez M, Bowman JL, Sundaresan V (2009) Auxin-dependent patterning and gamete specification in the *Arabidopsis* female gametophyte. *Science* 324:1684–1689.
23. Leydon AR, et al. (2013) Three MYB transcription factors control pollen tube differentiation required for sperm release. *Curr Biol* 23:1209–1214.
24. Liang Y, et al. (2013) MYB97, MYB101 and MYB120 function as male factors that control pollen tube-synergid interaction in *Arabidopsis thaliana* fertilization. *PLoS Genet* 9:e1003933.
25. Ingouff M, Hamamura Y, Gourgues M, Higashiyama T, Berger F (2007) Distinct dynamics of HISTONE3 variants between the two fertilization products in plants. *Curr Biol* 17:1032–1037.
26. Beale KM, Leydon AR, Johnson MA (2012) Gamete fusion is required to block multiple pollen tubes from entering an *Arabidopsis* ovule. *Curr Biol* 22:1090–1094.

27. Steffen JG, Kang IH, Macfarlane J, Drews GN (2007) Identification of genes expressed in the Arabidopsis female gametophyte. *Plant J* 51:281–292.
28. Park M, et al. (2013) *Arabidopsis* μ-adaptin subunit AP1M of adaptor protein complex 1 mediates late secretory and vacuolar traffic and is required for growth. *Proc Natl Acad Sci USA* 110:10318–10323.
29. Wang X, et al. (2014) *Trans*-Golgi network-located AP1 gamma adaptins mediate dileucine motif-directed vacuolar targeting in *Arabidopsis*. *Plant Cell* 26:4102–4118.
30. Chopin F, et al. (2007) The *Arabidopsis* ATNRT2.7 nitrate transporter controls nitrate content in seeds. *Plant Cell* 19:1590–1602.
31. Duan Q, Kita D, Li C, Cheung AY, Wu H-M (2010) FERONIA receptor-like kinase regulates RHO GTPase signaling of root hair development. *Proc Natl Acad Sci USA* 107:17821–17826.
32. Dettmer J, et al. (2005) Essential role of the V-ATPase in male gametophyte development. *Plant J* 41:117–124.
33. Strompen G, et al. (2005) Arabidopsis vacuolar H-ATPase subunit E isoform 1 is required for Golgi organization and vacuole function in embryogenesis. *Plant J* 41:125–132.
34. Hara-Nishimura I, Hatsugai N (2011) The role of vacuole in plant cell death. *Cell Death Differ* 18:1298–1304.
35. Kuroyanagi M, et al. (2005) Vacuolar processing enzyme is essential for mycotoxin-induced cell death in *Arabidopsis thaliana*. *J Biol Chem* 280:32914–32920.
36. Shen J, et al. (2013) Organelle pH in the *Arabidopsis* endomembrane system. *Mol Plant* 6:1419–1437.
37. Viotti C, et al. (2010) Endocytic and secretory traffic in *Arabidopsis* merge in the trans-Golgi network/early endosome, an independent and highly dynamic organelle. *Plant Cell* 22:1344–1357.
38. Kasahara RD, et al. (2012) Fertilization recovery after defective sperm cell release in *Arabidopsis*. *Curr Biol* 22:1084–1089.
39. Schumacher K, Krebs M (2010) The V-ATPase: Small cargo, large effects. *Curr Opin Plant Biol* 13:724–730.
40. Kriegel A, et al. (2015) Job sharing in the endomembrane system: Vacuolar acidification requires the combined activity of V-ATPase and V-PPase. *Plant Cell* 27: 3383–3396.
41. Zhou LZ, et al. (2013) Protein S-ACYL Transferase10 is critical for development and salt tolerance in *Arabidopsis*. *Plant Cell* 25:1093–1107.
42. Wang JG, et al. (2013) HAPLESS13, the Arabidopsis μ1 adaptin, is essential for protein sorting at the trans-Golgi network/early endosome. *Plant Physiol* 162:1897–1910.
43. Li S, et al. (2013) Arabidopsis COBRA-LIKE 10, a GPI-anchored protein, mediates directional growth of pollen tubes. *Plant J* 74:486–497.
44. Karimi M, Inzé D, Depicker A (2002) GATEWAY vectors for *Agrobacterium*-mediated plant transformation. *Trends Plant Sci* 7:193–195.
45. Guo J, Wang F, Song J, Sun W, Zhang XS (2010) The expression of *Orysa;CycB1;1* is essential for endosperm formation and causes embryo enlargement in rice. *Planta* 231:293–303.